Beam Quality of a Nonideal Atom Laser

J.-F. Riou,* W. Guerin, Y. Le Coq,† M. Fauquembergue, V. Josse, P. Bouyer, and A. Aspect

Laboratoire Charles Fabry de l'Institut d'Optique, Centre National de la Recherche Scientifique et Université Paris Sud 11, Bât. 503, Campus Universitaire d'Orsay, 91403 Orsay Cedex, France

(Received 11 September 2005; published 24 February 2006)

We study the propagation of a noninteracting atom laser distorted by the strong lensing effect of the Bose-Einstein condensate (BEC) from which it is outcoupled. We observe a transverse structure containing caustics that vary with the density within the residing BEC. Using the WKB approximation, Fresnel-Kirchhoff integral formalism, and *ABCD* matrices, we are able to describe analytically the atom-laser propagation. This allows us to characterize the quality of the nonideal atom-laser beam by a generalized M^2 factor defined in analogy to photon lasers. Finally we measure this quality factor for different lensing effects.

DOI: 10.1103/PhysRevLett.96.070404 PACS numbers: 03.75.Pp, 39.20.+q, 41.85.Ew, 42.60.Jf

Optical lasers have had an enormous impact on science and technology, due to their high brightness and coherence. The high spatial quality of the beam and the little spread when propagating in the far-field enable applications ranging from the focusing onto tiny spots and optical lithography [1] to collimation over astronomic distances [2]. In atomic physics, Bose-Einstein condensates (BECs) of trapped atoms [3] are an atomic equivalent to photons stored in a single mode of an optical cavity, from which a coherent matter wave (atom laser) can be extracted [4,5]. The possibility of creating a continuous atom laser [6] promises spectacular improvements in future applications [7–11] where perfect collimation or strong focusing [12–14] are of prior importance. Nevertheless, these properties depend drastically on whether the diffraction limit can be achieved. Thus, characterizing the deviation from this limit is, as for optical lasers [15], of crucial importance. For example, thermal lensing effects in optical laser cavities, which cause significant decollimation, can also induce aberrations that degrade the transverse profile. In atom optics, a trapped BEC weakly interacting with the outcoupled atom-laser beam acts as an effective thin lens which leads to the divergence of the atom laser [16] without affecting the diffraction limit. When the lensing effect increases, dramatic degradations of the beam are predicted [17], with the apparition of caustics on the edge of the beam.

In order to quantitatively qualify the *atom-laser beam quality*, it is tempting to take advantage of the methods developed in optics to deal with nonideal laser beams, i.e., above the diffraction limit. Following the initial work of Siegman [18] who introduced the quality factor M^2 which is proportional to the space-beam-width (divergence $\times$ size) product at the waist, it is natural to extend its definition to atom optics as

$$\Delta x \Delta k_x = \frac{M^2}{2}, \tag{1}$$

where Δx and $\Delta k_x = \Delta p_x/\hbar$ characterize, respectively, the size and the divergence along x (Δp_x is the width of the momentum distribution). Equation (1) plays the same role as the Heisenberg dispersion relation: it expresses how many times the beam deviates from the diffraction limit.

In this Letter, we experimentally and theoretically study the quality factor M^2 of a nonideal, noninteracting atom-laser beam. First, we present our experimental investigation of the structures that appear in the transverse profile [19]. We show that they are induced by the strong lensing effect due to the interactions between the trapped BEC and the outcoupled beam. Then, using an approach based on

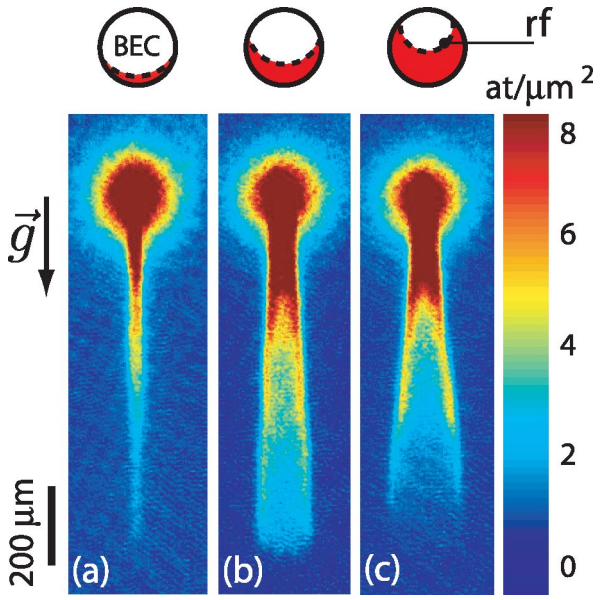

FIG. 1 (color). Absorption images of a nonideal atom laser, corresponding to density integration along the elongated axis of the BEC. The figures correspond to different height of rf outcoupler with respect to the bottom of the BEC: (a) 0.37 μm, (b) 2.22 μm, (c) 3.55 μm. The graph above shows the rf outcoupler (dashed line) and the BEC slice (red) which is crossed by the atom laser. This results in the observation of caustics. The field of view is 350 μm $\times$ 1200 μm for each image.

the WKB approximation and the Fresnel-Kirchhoff integral formalism, we are able to calculate analytical profiles which agree with our experimental observations. This allows us to generalize concepts introduced in [18] for photon laser and to calculate the quality factor M^2. This parameter can then be used in combination with the paraxial $ABCD$ matrices [20] to describe the propagation of the nonideal beam via the evolution of the rms width. Finally, we present a study of the M^2 quality factor as a function of the thickness of the BEC-induced output lens.

Our experiment produces atom lasers obtained by radio frequency (rf) outcoupling from a BEC [5,21]. The experimental setup for creating condensates of ^{87}Rb is described in detail in [22]. Briefly, a Zeeman-slowed atomic beam loads a magneto-optical trap in a glass cell. About 2×10^8 atoms are transferred in the $|F, m_F\rangle = |1, -1\rangle$ state to a Ioffe-Pritchard magnetic trap, which is subsequently compressed to oscillation frequencies of $\omega_y = 2\pi \times 8$ Hz and $\omega_{x,z} = 2\pi \times 330$ Hz in the dipole and quadrupole directions, respectively. A 25 s rf induced evaporative cooling ramp results in a pure condensate of $N = 10^6$ atoms, cigar-shaped along the y axis.

The atom laser is extracted from the BEC by applying a rf field a few kHz above the bottom of the trap, in order to couple the trapped state to the weakly antitrapped state $|1, 0\rangle$. The extracted atom-laser beam falls under the effect of both gravity $-mgz$ and second order Zeeman effect $V = -m\omega^2(x^2 + z^2)/2$ [23] with $\omega = 2\pi \times 20$ Hz [see Fig. 2(a)]. The rf outcoupler amplitude is weak enough to avoid perturbation of the condensate so that the laser dynamics is quasistationary [21] and the resulting atom flux is low enough to avoid interactions within the propagating beam. Since the BEC is displaced vertically by the gravitational sag, the value of the rf outcoupler frequency ν_{rf} defines the height where the laser is extracted [5]. After 10 ms of operation, the fields are switched off and absorption imaging is taken after 1 ms of free fall with a measured spatial resolution of 6 μm. The line of sight is along the weak y axis so that we observe the transverse profile of the atom laser in the (z, x) plane.

Typical images are shown in Fig. 1. Transverse structures, similar to the predictions in [17], are clearly visible in Figs. 1(b) and 1(c). The laser beam quality degrades as the rf outcoupler is higher in the BEC (i.e., the laser beam crosses more condensate), supporting the interpretation that this effect is due to the strong repulsive interaction between the BEC and the laser. This effect can be understood with a semiclassical picture. The mean-field interaction results in an inverted harmonic potential of frequencies ω_i (in the directions $i = x, y, z$) which, in the Thomas-Fermi regime, are fixed by the magnetic confinement [16,24]. The interaction potential expels the atoms transversally, as illustrated in Fig. 2(b). Because of the finite size of the condensate, the trajectories initially at the center of the beam experience more mean-field repulsion than the ones initially at the border. This results in accumulation of trajectories at the edge of the atom-laser beam [17], in a similar manner to caustics in optics. This picture enables a clear physical understanding of the behavior observed in Fig. 1: if ν_{rf} is chosen so that extraction is located at the bottom of the BEC [Fig. 1(a)], the lensing effect is negligible and one gets a collimated beam. As the rf outcoupler moves upwards [Figs. 1(b) and 1(c)], a thicker part of the condensate acts on the laser and defocusing, then caustics appear. We verified that when sufficiently decreasing the transverse confinement of the trapped BEC, i.e., making the interaction with the outcoupled atoms negligible, the atom laser is collimated at any rf value [25].

In order to describe quantitatively the details of the profiles of the nonideal atom laser one could solve numerically the Gross-Pitaevskii equation (GPE) [17,19]. As we show here, another approach is possible, using approximations initially developed in the context of photon optics and extended to atom optics. These approximations allow calculation of the atom-laser propagation together with the characterization of its rms width evolution by means of the quality factor M^2, in combination with $ABCD$ matrices. Note, however, that these matrices can only be used in the paraxial regime, i.e., when the transverse kinetic energy is smaller than the longitudinal one [16]. This condition does not hold in the vicinity of the BEC, and thus we split the atom-laser evolution into three steps [Fig. 2(b)] where we use different formalisms in close analogy with optics: (I) WKB inside the condensate (eikonal), (II) Fresnel-Kirchhoff integral outside the con-

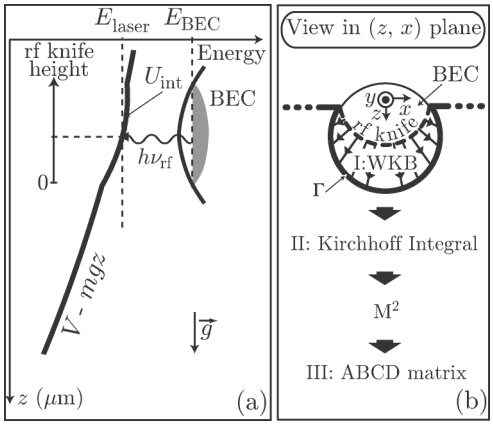

FIG. 2. (a) Principle of the rf outcoupler: the radio frequency $\nu_{\mathrm{rf}} = (E_{\mathrm{BEC}} - E_{\mathrm{laser}})/h$ selects the initial position of the extracted atom-laser beam. The laser is then subjected to the condensate mean-field potential U_{int}, to the quadratic Zeeman effect V, and to gravity $-mgz$. For the sake of clarity, V has been exaggerated on the graph. (b) Representation of the two-dimensional theoretical treatment: (I) inside the condensate, phase integral along atomic paths determines the laser wave front at the BEC output (WKB approximation). (II) A Fresnel-Kirchhoff integral on the contour Γ is used to calculate the stationary laser wave function at any point below the condensate. (III) As soon as the beam enters the paraxial regime, we calculate the M^2 quality factor and use $ABCD$ matrix formalism.

densate and, (III) paraxial *ABCD* matrices after sufficient height of fall. In all the following, we do not include interactions within the atom laser since they are negligible for the very dilute beam considered in this Letter. In addition, the condensate is elongated along the y axis, so that the forces along this direction are negligible and we consider only the dynamics in the (z, x) plane.

First, we consider that the atoms extracted from the condensate by the rf outcoupler start at zero velocity from $\mathbf{r}_0$. In region (I) the total potential (resulting from gravity and interactions with the trapped BEC) is cylindrically symmetric along the y axis. The trajectories are thus straight lines [see Fig. 2(b)]. The beam profile $\psi(\mathbf{r}_1)$ at the BEC border is obtained thanks to the WKB approximation, by integrating the phase along classical paths of duration τ_0

$$\psi(\mathbf{r}_1) \propto \frac{1}{\sqrt{\sinh(2\omega_z\tau_0)}} e^{i\int_{\mathbf{r}_0}^{\mathbf{r}_1}\mathbf{k}(\mathbf{r})\cdot d\mathbf{r}}\psi_{\mathrm{BEC}}(\mathbf{r}_0), \qquad (2)$$

where ψ_{BEC} is the condensate wave function and the prefactor ensures the conservation of the flux.

The atom laser being in a quasistationary state, the wave function satisfies in region (II) the time-independent Schrödinger equation at a given energy E in the potential $V - mgz$. Since this equation is analogous to the Helmoltz equation [26,27] in optics, the Fresnel-Kirchhoff integral formalism can be generalized to atom optics as [28]

$$\psi(\mathbf{r}) \propto \oint_\Gamma d\boldsymbol{l} \cdot [G_E \nabla_1 \psi(\mathbf{r}_1) - \psi(\mathbf{r}_1)\nabla_1 G_E]. \qquad (3)$$

We take the contour Γ along the condensate border and close it at infinity [see Fig. 2(b)]. The time-independent Green's function $G_E(\mathbf{r}, \mathbf{r}_1)$ is analytically evaluated from the time-domain Fourier transform of the Feynman propagator $K(\mathbf{r}, \mathbf{r}_1, \tau)$ [28,29] calculated by means of the van Vleck formula [30]. Using $\psi(\mathbf{r}_1)$ from Eq. (2), the wave function $\psi(\mathbf{r})$ is then known at any location $\mathbf{r}$. We verified the excellent agreement of this model with a numerical integration of the GPE including intralaser interactions, thus confirming that they remain negligible throughout propagation.

The method using a Kirchhoff integral is demanded only for the early stages of the propagation. As soon as the paraxial approximation becomes valid, the *ABCD* matrix formalism can be used to describe the propagation of the beam. An example of a profile calculated in the central plane ($y = 0$) is presented in Fig. 3(a). In Fig. 3(b) we add the profiles of all y planes, taking into account the measured resolution of the imaging system. In Fig. 3(c) we present the corresponding experimental profile. The overall shape is in good agreement with theory, and the differences can be explained by imperfections in the imaging process and bias fluctuations during outcoupling. The rms size of the three profiles, which depend very smoothly on the details of the structure, are the same within experimental uncertainties. Thus, hereafter, as in the case of propagation of optical laser using the M^2 parameter, we only consider the evolution of the rms size of the atom laser.

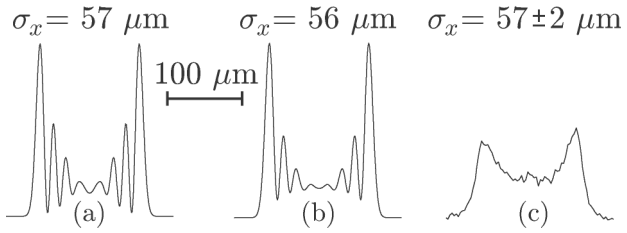

FIG. 3. Beam profile after 600 μm of propagation for an outcoupler height of 3.55 μm: (a) calculated in the central plane $y = 0$, (b) resulting from the integration along the line of sight y, (c) obtained experimentally. Deviations between the curves (b) and (c) can be attributed to imperfections in the imaging process and bias fluctuations. Note that for all three profiles, the overall shape is preserved and the calculated rms width in the central plane is in agreement with the measured one within experimental errors.

To calculate the beam width change in the paraxial regime, we define, following [18], a generalized complex radius of curvature

$$\frac{1}{q(\xi)} = C(\xi) + \frac{iM^2}{2\sigma_x^2(\xi)}, \qquad (4)$$

where σ_x is the rms width of the density profile and $\xi(t)$ a reduced variable which describes the time evolution of the beam such that $\xi = 0$ corresponds to the position of the waist. Equation (4) involves an invariant coefficient, the beam-quality factor M^2, as defined in Eq. (1). This coefficient, as well as the effective curvature $C(\xi)$, can be extracted from the wave front in the paraxial domain, as explained in [31]. In optics, the generalized complex radius obeys the same *ABCD* propagation rules as does a Gaussian beam of the same real beam size, if the wavelength λ is changed to $M^2\lambda$ [20]. Similarly, the complex radius $q(\xi)$ follows here the *ABCD* law for matter waves [16], and we obtain the rms width

$$\sigma_x^2(\xi) = \sigma_{x0}^2 \cosh^2(\xi) + \left(\frac{M^2\hbar}{2m\omega}\right)^2 \frac{\sinh^2(\xi)}{\sigma_{x0}^2}, \qquad (5)$$

where σ_{x0} is taken at the waist.

This generalized Rayleigh formula allows us to measure M^2. In the inset of Fig. 4, the evolution of the transverse rms width σ_x versus propagation ξ, taken from experimental images, is compared to the one given by Eq. (5), where σ_{x0} is calculated with our model. For a chosen rf outcoupler position, we fit the variation of the width with a single free parameter M^2. We then plot the measured value of M^2 versus the ouput coupler height (Fig. 4), and we find good agreement with theory.

In conclusion, we have characterized the transverse profile of an atom laser. We demonstrated that, in our case, lensing effect when crossing the condensate is a critical contributor to the observed degradation of the

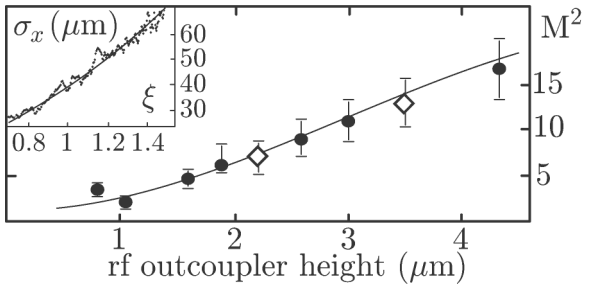

FIG. 4. M^2 quality factor vs rf outcoupler distance from the bottom of the BEC: theory (solid line), experimental points (circles). The two diamonds represent the M^2 for the two non-ideal atom lasers shown in Figs. 1(b) and 1(c). The rf outcoupler position is calibrated by the number of outcoupled atoms. Inset: typical fit of the laser rms size with the generalized Rayleigh formula [Eq. (5)] for rf outcoupler position 3.55 μm.

beam. We showed that the beam-quality factor M^2, initially introduced by Siegman [18] for photon laser, is a fruitful concept for describing the propagation of an atom-laser beam with *ABCD* matrices, as well as for characterizing how far an atom laser deviates from the diffraction limit. For instance, it determines the minimal focusing size that can be achieved with atomic lenses provided that interactions in the laser remain negligible [14,32]. This is of essential importance in view of future applications of coherent matter waves as, for example, when coupling atom lasers onto guiding structures of atomic chips [33]. In addition, if interactions within atom laser become non-negligible, a further treatment could be developed in analogy with the work of [34] for nonlinear optics.

The authors would like to thank S. Rangwala, A. Villing, and F. Moron for their help on the experiment, L. Sanchez-Palencia and I. Bouchoule for fruitful discussions, and R. Nyman for careful reading of the manuscript. This work is supported by CNES (DA:10030054), DGA (Contracts No. 9934050 and No. 0434042), LNE, EU (Grants No. IST-2001-38863, No. MRTN-CT-2003-505032, and No. FINAQS STREP), INTAS (Contract No. 211-855), and ESF (BEC2000+).

*Email address: Jean-Felix.Riou@iota.u-psud.fr
Electronic address: http://atomoptic.iota.u-psud.fr
†Present address: NIST, Mailcode 847.10, 325 Broadway, Boulder, CO 80305-3328, USA.

[1] R. Ito and S. Okazaki, Nature (London) **406**, 1027 (2000).
[2] P. L. Bender *et al.*, Science **182**, 229 (1973).
[3] M. H. Anderson *et al.*, Science **269**, 198 (1995); K. B. Davis *et al.*, Phys. Rev. Lett. **75**, 3969 (1995); C. C. Bradley, C. A. Sackett, J. J. Tollett, and R. G. Hulet, Phys. Rev. Lett. **75**, 1687 (1995).
[4] M.-O. Mewes *et al.*, Phys. Rev. Lett. **78**, 582 (1997); B. P. Anderson *et al.*, Science **282**, 1686 (1998); E. W. Hagley *et al.*, Science **283**, 1706 (1999).
[5] I. Bloch, T. W. Hänsch, and T. Esslinger, Phys. Rev. Lett. **82**, 3008 (1999).
[6] A. P. Chikkatur *et al.*, Science **296**, 2193 (2002); T. Lahaye *et al.*, Phys. Rev. A **72**, 033411 (2005).
[7] P. Bouyer and M. A. Kasevich, Phys. Rev. A **56**, R1083 (1997).
[8] Y.-J. Wang *et al.*, Phys. Rev. Lett. **94**, 090405 (2005).
[9] Y. Shin *et al.*, Phys. Rev. A **72**, 021604(R) (2005).
[10] E. te Sligte *et al.*, Appl. Phys. Lett. **85**, 4493 (2004); G. Myszkiewicz *et al.*, Appl. Phys. Lett. **85**, 3842 (2004).
[11] Y. Le Coq *et al.*, cond-mat/0501520.
[12] I. Bloch, M. Kohl, M. Greiner, T. W. Hansch, and T. Esslinger, Phys. Rev. Lett. **87**, 030401 (2001).
[13] I. Shvarchuck *et al.*, Phys. Rev. Lett. **89**, 270404 (2002).
[14] A. S. Arnold, C. MacCormick, and M. G. Boshier, J. Phys. B **37**, 485 (2004).
[15] A. E. Siegman, in *Solid State Lasers: New Developments and Applications*, edited by M. Inguscio and R. Wallenstein (Plenum, New York, 1993), p. 13.
[16] Y. Le Coq *et al.*, Phys. Rev. Lett. **87**, 170403 (2001).
[17] T. Busch, M. Kohl, T. Esslinger, and K. Molmer, Phys. Rev. A **65**, 043615 (2002).
[18] A. E. Siegman, IEEE J. Quantum Electron. **27**, 1146 (1991).
[19] Similar observations had been reported in M. Köhl *et al.*, Phys. Rev. A **72**, 063618 (2005).
[20] P. A. Bélanger, Opt. Lett. **16**, 196 (1991).
[21] F. Gerbier, P. Bouyer, and A. Aspect, Phys. Rev. Lett. **86**, 4729 (2001); Phys. Rev. Lett. **93**, 059905(E) (2004).
[22] M. Fauquembergue *et al.*, Rev. Sci. Instrum. **76**, 103104 (2005).
[23] B. Desruelle *et al.*, Phys. Rev. A **60**, R1759 (1999).
[24] F. Dalfovo *et al.*, Rev. Mod. Phys. **71**, 463 (1999).
[25] We also verified that the lensing effect varies very little with condensate atom number since the Thomas-Fermi radius, and thus the part acting on the atom laser varies as $N^{1/5}$ [24].
[26] M. Born and E. Wolf, *Principles of Optics* (Cambridge University Press, Cambridge, England, 2002), 7th ed.
[27] C. Henkel, J.-Y. Courtois, and A. Aspect, J. Phys. II **4**, 1955 (1994).
[28] Ch. J. Bordé in *Fundamental Systems in Quantum Optics*, edited by J. Dalibard (Elsevier, New York, 1991); Ch. J. Bordé, C. R. Acad. Sci. Paris, t. 2, Série IV 509 (2001).
[29] R. P. Feynman and A. R. Hibbs, *Quantum Mechanics and Path Integrals* (McGraw-Hill, New York, 1965).
[30] J. H. van Vleck, Proc. Natl. Acad. Sci. U.S.A. **14**, 178 (1928).
[31] A. E. Siegman, *Lasers* (University Science Books, Mill Valley, California, 1986).
[32] For a focusing size R the transverse kinetic energy deduced from Eq. (1) is $(M^2)^2\hbar^2/4mR^2$, whereas the interaction energy reads $2\pi\hbar^2 a\mathcal{F}/vmR^2$, with a, v, and $\mathcal{F}$ being respectively the scattering length, the on-axis beam velocity, and the flux. Interactions are thus negligible if $\mathcal{F}/v \ll (M^2)^2/8\pi a$.
[33] See special issue on "Atom Chips: Manipulating Atoms and Molecules with Microfabricated Structures," edited by C. Henkel, J. Schmiedmayer, and C. Westbrook [Eur. Phys. J. D 35, No. 1 (2005)].
[34] C. Paré and P. A. Bélanger, Opt. Quantum Electron. **24**, S1051 (1992).